Chinese Chemical Letters 32 (2021) 397–400

Contents lists available at ScienceDirect

Chinese Chemical Letters

journal homepage: www.elsevier.com/locate/cclet

Communication

Super rigid tris-spirobifluorenes: Syntheses and properties

Luyao Zhao[a,b,1], Chunbo Duan[c,1], Dongxue Ding[c,1], Shihui Liu[b], Debin Xia[b,*], Ying Guo[a,*], Hui Xu[c,*], Martin Baumgarten[d]

[a] College of Chemical and Environmental Engineering, Harbin University of Science and Technology, Harbin 150040, China
[b] MIIT Key Laboratory of Critical Materials Technology for New Energy Conversion and Storage, School of Chemistry and Chemical Engineering, Harbin Institute of Technology, Harbin 150001, China
[c] Key Laboratory of Functional Inorganic Material Chemistry, Ministry of Education, School of Chemistry and Material Science, Heilongjiang University, Harbin 150080, China
[d] Max Planck Institute for Polymer Research, Mainz 55128, Germany

ARTICLE INFO

Article history:
Received 22 December 2019
Received in revised form 13 January 2020
Accepted 2 February 2020
Available online 5 February 2020

Keywords:
OLEDs
Spirobifluorene
Blue emitter
Rigid structure
Three dimensional

ABSTRACT

In this work, a blue emitter with a 3D rigid structure composed of multiple spirobifluorene (**3-Spiro**) has been synthesized and characterized. Through a detailed study of the electrochemical and photophysical properties of **3-Spiro**, we have evidenced that **3-Spiro** can be applied as an active component of organic light-emitting diodes (OLEDs). The device with 5% doping rate of 4CzPNPh exhibits high external quantum efficiency (EQE) of 11%, which proves the potential of 3D rigid structure emitters for OLEDs.

As the next-generation display technology, organic light-emitting diodes (OLEDs) have the characteristics of self-illumination, low power consumption and flexible, making their market value huger in 5 G era [1–4]. However, with respect to red and green emitters, blue emitters must be invented to produce white light sources [5,6]. It is a big challenge to develop blue counterparts with excellent efficiency and color purity, because of the intrinsic wide gap, which prevents efficient charges from being injected into the emitting layer. Therefore, from a commercialization viewpoint, it is imperative to design and synthesis high-performance blue-emitting materials [7–11].

Spirobifluorene is nowadays an important building block for blue-emitting materials due to its high photoluminescence quantum yield (PLQY) [12–14]. There are abundant examples of efficient spirobifluorene-based materials [15]. Nevertheless, linkages between spirobifluorenes in almost all the blue-emitting materials are by single bonds or flexible segments [16–20]. As far as we know spirobifluorene-based rigid molecules are rarely reported [21].

With the aim of building novel emitters with good thermal stability and excellent color purity, together with relatively high photoluminescence quantum yields, we designed and synthesized a 3D rigid blue emitter with three spirobifluorene units on the basis of the dihydroindenofluorene (Scheme 1). The compound named **3-Spiro** is expected to have the following properties: (1) the "super-rigid" structure facilitates the enhancement of thermal stability, and the decrease of Stokes shift; (2) large steric hindrance can effectively suppress aggregation-induced self-quenching, enabling material to present relatively high PLQY [22,23].

Herein, we present the synthesis and characterization of a 3D rigid blue emitter **3-Spiro** with three spirobifluorene units. Its electrochemical, photophysical properties and thermal stability were analyzed. Finally, we investigated the performance of **3-Spiro** in blue OLEDs.

The synthetic route to **3-Spiro** is presented in Scheme 1. The starting material **2O-Spiro** was prepared according to our previous work [24].

3-Spiro was synthesized *via* a nucleophilic reaction between **2O-Spiro** and [1,1′-biphenyl]-2-ylmagnesium bromide, followed by an intramolecular cyclization reaction under the reflux condition using acetic acid as solvent. To obtain high reaction yield, 10 equiv. of 2-bromobiphenyl was used, which ensured the complete nucleophilic substitution. Therefore, 92% reaction yield was achieved. Moreover, the compound **3-Spiro** can be further

* Corresponding authors.
E-mail addresses: xia@hit.edu.cn (D. Xia), gyingxinxiang@126.com (Y. Guo), hxu@hlju.edu.cn (H. Xu).
[1] These authors contributed equally to this work.

https://doi.org/10.1016/j.cclet.2020.02.001
1001-8417/

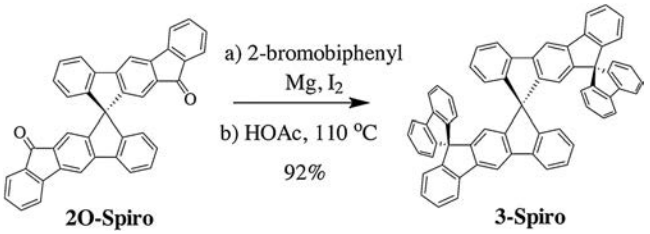

Scheme 1. Synthesis of **3-Spiro**.

converted to tris-spirobifluorenes-2-iodoacetophenone (**3-Spiro**-I) (chemical structure and single crystal structure were shown in Fig. S1 in Supporting information) *via* Friedel-Crafts reaction with 2-iodobenzoyl chloride. By altering the amount of 2-iodobenzoyl chloride addition, the formation of mono-, di- or multi-2-iodobenzoyl **3-Spiro** can be reached. Thus it is expected to form novel rigid oligofluorenes with multiple spiro-connection *via* our reported strategy (Fig. S1). [24]

The chemical structure of **3-Spiro** was unambiguously proved by NMR spectroscopy, MALDI-TOF mass and single crystal X-ray diffraction. After 2D NMR analysis, which included H-C HMBC, H-H NOESY, H-H COSY and H-H TOCSY, the different protons within the molecule can be assigned. Firstly, HMBC spectrum (Fig. S2 in Supporting information) was performed to investigate correlations between spiro carbons and their neighboring hydrogens. Consequently, H_A and H_B are assigned to the single peak with the chemical shift of 6.09 ppm and double peaks with the chemical shift of 6.62 ppm, respectively. Obviously, the other single peak (8.26 ppm) is ascribed to proton H_F. Thereafter, H_G and H_E can also be assigned to the double peaks with chemical shifts of 7.95 and 7.90 ppm, respectively, since both protons have correlations with H_F in the NOESY spectrum (Fig. S3 in Supporting information) and only proton H_E has correlation with known H_B in the TOCSY spectrum (Fig. S4 in Supporting information). Through the COSY spectrum (Fig. S5 in Supporting information), the assignment of H_H (7.39 ppm) and H_J (6.53 ppm) protons on the dihydroindeno[2,1-*b*] fluorenyl moieties is straightforward. Regarding the H_C, H_D and H_I, their peaks are mixed with the peaks arising from protons of two fluorene units. Unfortunately, the attempt to specify the proton positions of fluorene was failed. The thermal stability of **3-Spiro** was revealed by thermogravimetric analysis (TGA), which exhibited an excellent thermal stability at 450 °C with 5% weight loss (Fig. S6 in Supporting information).

To further understand the intermolecular interactions in the solid state, single crystals of **3-Spiro** for X-ray diffraction analysis were successfully obtained by slow evaporation of the hexane and dichloromethane mixed solution for **3-Spiro**. As shown in Fig. 1, **3-Spiro** presents the rigid three-dimensional structure, which could efficiently prevent the intermolecular self-aggregation and thus reduce or eliminate the quenching of the luminance. The

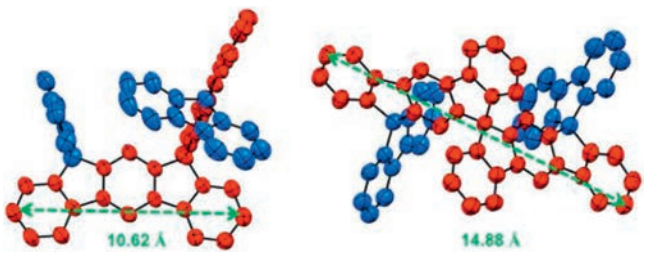

Fig. 1. X-ray diffraction structure of **3-Spiro**. Hydrogen atoms are omitted for clarity.

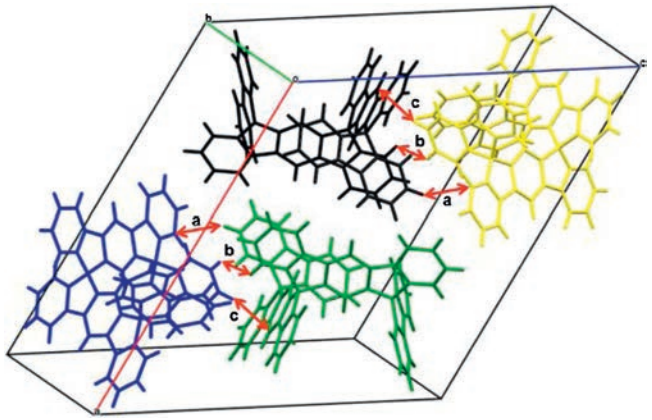

Fig. 2. X-ray diffraction structure of **3-Spiro**. Intermolecular distances: a: 2.88 Å (C···H); b: 2.29 Å (H···H); c: 2.80 Å (C···H).

dihydroindeno[2,1-*b*]fluorenyl core of **3-Spiro** has a maximum length of 10.6 Å. The diameter of the molecule is up to14.88 Å (right in Fig. 1). As shown in Fig. 2, three types of intermolecular interactions in different directions are observed, namely, C···H (a), H···H (b) and C···H (c), with a distance of 2.88 Å, 2.29 Å and 2.80 Å, respectively. Surprisingly, no intermolecular π–π interaction is observed in such crystals, even though large planar aromatic rings, such as fluorene and dihydroindeno [2,1-*b*]fluorenyl core exist in this system. That can be explained by the steric hindrance effect.

To have a better understanding of the photophysical properties of **3-Spiro**, UV–vis absorption and emission spectroscopy were employed. As shown in Fig. 3, UV–vis absorption spectrum of **3-Spiro** (in CH_2Cl_2) exhibits six characteristic bands (269, 297, 311, 328, 334 and 344 nm) that are very similar to those previously observed for its analogue, such as dihydroindeno[1,2-*b*]fluorene (chemical structure shown in Fig. S7 in Supporting information) [25]. The absorption bands of **3-Spiro** in the thin film spectrum are only slightly red-shifted (4 nm) compared to that in solution. Moreover, in the case of **3-Spiro**, two emission bands in CH_2Cl_2 were observed. The emission spectrum is well-resolved with a main band at 351 nm and thus with a narrow Stokes shift of 8 nm. This is indicative of an extremely rigid chromophore, in which the vibrational relaxation of the excited state is dramatically restricted. The feature is also related to the high quantum yield of approximately 0.45, especially for the violet emitter, which could also be used as host for the sky-blue emitting phosphorescent material. In the neat film, however, the emission behavior is different. In the solid state, **3-Spiro** displays a red shift of about

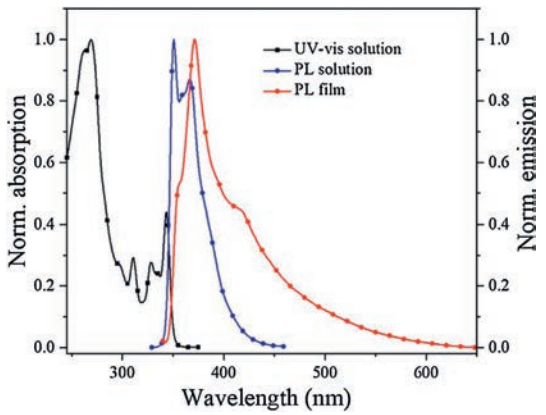

Fig. 3. Absorption (square) and photoluminescence (cycle) spectra of **3-Spiro** in DCM (λ_{Exc} = 330 nm) and thin film (λ_{Exc} = 270 nm).

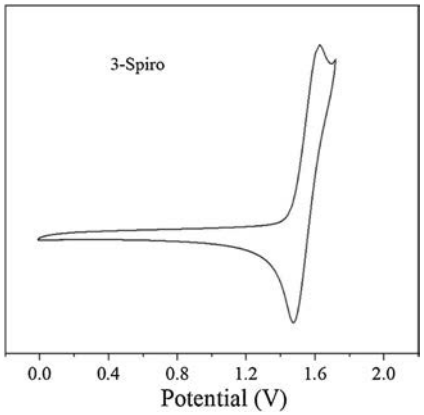

Fig. 4. Cyclic voltammetric profile of **3-Spiro** in dichloromethane at a scan rate of 100 mV/s with 0.1 mol/L Bu_4NPF_6 as supporting electrolyte.

20 nm, together with the appearance of a long tail in the range of λ = 400−600 nm. This indicates the existence of strong intermolecular interactions in the solid state. To prevent this phenomenon in the future, more bulk groups, such as dendrimer, could be introduced in the core.

To design the configuration of the OLED devices with high emitting efficiency, it is essential to determine the HOMO and LUMO energy levels of the chromophore in the emissive layer (EML). Thus, redox behavior of **3-Spiro** was investigated by cyclic voltammetry (CV). Cyclic voltammograms (Fig. 4) of **3-Spiro** in DCM exhibits only one oxidation wave, with the $E_{1/2}$ potential around 1.54 V, arising from the oxidation of the dihydroindenofluorenyl units. The HOMO energy level estimated through the equation $E_{HOMO} = -[E_{oxd1/2} - E_{(Fc+/Fc)} + 4.8]$ eV is around −5.84 eV. However, in the accessible potential range, we have not observed the reduction wave. The LUMO energy is calculated from the optical gap to be -2.30 eV, according to the equation LUMO = HOMO + E_g. The optical gap was calculated from the onset of the absorption spectrum. Thereafter, materials for hole and electron transporting layers can be chosen for efficient charge carrier transfer from the electrodes to the EML.

In order to gain more insight into the optoelectronic characteristics of **3-Spiro**, density functional theory (DFT) calculations were performed. In Figs. S8 and S9 (Supporting information), the HOMO and LUMO are mainly located on dihydroindenofluorene units, with the energy levels of −5.63 and −1.36 eV, respectively. This indicates that the spiro linkage can keep the original properties of its connected fragments. Ongoing from HOMO to HOMO-1 and HOMO-2, the dispersion of electron cloud densities increased to fluorene moieties correspondingly. Simultaneously, the energy levels of occupied molecular orbitals HOMO-1 and HOMO-2 are decreased to −5.87 eV and −6.12 eV, respectively. The energy levels of its LUMO and LUMO + 1 are almost degenerated, in which the electron density extends exclusively along the dihydroindenofluorene units. In LUMO + 2, small amount of electron dispersion on fluorene can be observed. This feature clearly indicates the main involvement of the dihydroindenofluorene fragments for electron injection in devices. The T1 energy levels of **3-Spiro** was estimated as the energy gaps between its ground state and T1 excited state to be 3.19 eV, which is around 0.30 eV higher than that of the traditional used host *N*,*N*′-dicarbazolyl-3,5-benzene (mCP). That indicates **3-Spiro** expands the varieties of being used as host for other blue-emitting materials with high triplet energies.

Finally, to evaluate the performance of **3-Spiro**, we investigated the complementary emitting devices with a bi-EML configuration of ITO/MoO_3 (6 nm)/NPB (70 nm)/mCP (5 nm)/**3-Sprio**:4CzPNPh (5 wt%, 20 nm)/**3-Sprio** (5 nm)/TPBI (30 nm)/LiF (1 nm)/Al, as shown in Fig. 5a. The yellow emitter 3,4,5,6-tetrakis(3,6-diphenyl-carbazol-9-yl)-1,2-dicyanobenzene (4CzPNPh) was employed as a dopant, since the emission spectrum of **3-Spiro** largely overlaps with the absorption spectrum of 4CzPNPh, allowing energy transfer. As shown in Fig. S10 (Supporting information), blue and yellow emission peaks are observed. The main peak around 400 nm correspond to the blue light, and the relative intensity of the blue component is voltage dependent. The device has a maximum current efficiency (CE) of 32.5 Cd/A, a maximum power efficiency (PE) of 15.3 Im/W, and an external quantum efficiency (EQE) of 11% (Figs. 5b and c). Simultaneously, we tested the device with 0.5% doping rate of 4CzPNPh. As shown in Fig. S11 (Supporting information), the 4CzPNPh doping

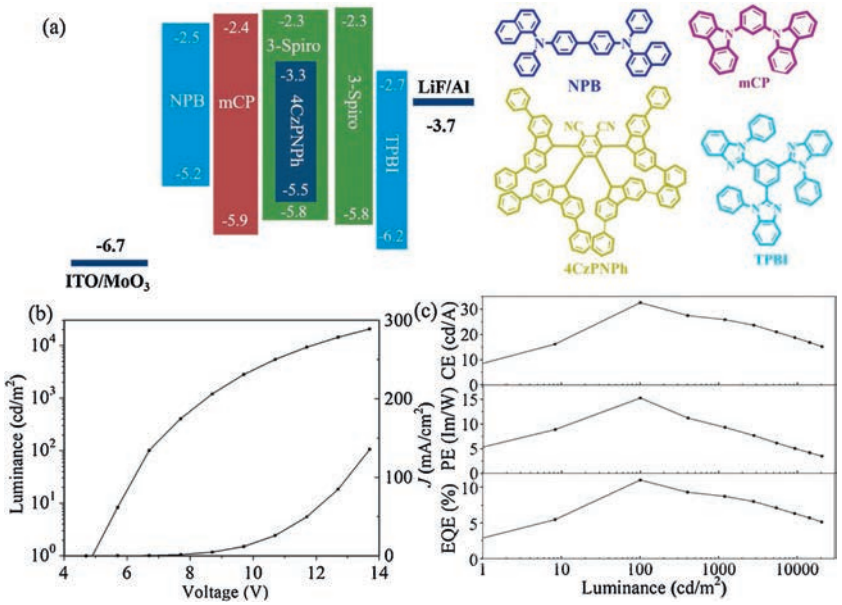

Fig. 5. (a) Device configuration and energy level diagram of **3-Spiro** and 4CzPNPh-based diodes, and chemical structures of the employed materials. (b) Luminance–current density and (J)–voltage characteristics. (c) Efficiency luminance correlations of the devices.

concentration does not affect the peak positions of **3-Spiro** and 4CzPNPh, whereas the efficiency is significantly lower than the former (Fig. S12 in Supporting information).

In conclusion, we have successfully designed and synthesized a rigid multiple spirobifluorenebased blue emitter (**3-Spiro**). It shows high thermal stability and photoluminescence quantum yields, which is strongly related to its rigid structure and large steric hindrance. Organic light-emitting diodes based on **3-Spiro** have been investigated and provided high external quantum efficiency (EQE) of 11%. Investigation into organic light-emitting diodes based on bigger rigid structures formed by **3-Spiro** expansion are ongoing in our laboratory, we believe that spirobifluorene family could play an indispensable role in the future.

Declaration of competing interest

The authors declare that they have no known competing financial interests or personal relationships that could have apperred to influence the work reported in this paper.

Acknowledgments

This work was supported by the National Natural Science Foundation of China (No. 51603055), the Natural Science Foundation of Heilongjiang Province (No. QC2017055), the China Postdoctoral Science Foundation (Nos. 2016M601424, 2017T100236), and the Postdoctoral Foundation of Heilongjiang Province (Nos. LBH-Z16059, LBH-TZ10).

Appendix A. Supplementary data

Supplementary material related to this article can be found, in the online version, at doi:https://doi.org/10.1016/j.cclet.2020.02.001.

References

[1] S. Ohisa, T. Takahashi, M. Igarashi, et al., Adv. Funct. Mater. 29 (2019) 1808022.
[2] Q. Li, S. Bi, J. Na, et al., ACS Nano 13 (2019) 8425–8432.
[3] Y. Zou, S. Gong, C. Yang, et al., Adv. Optical Mater. 6 (2018) 1800568.
[4] G. Zhang, Y. Li, C. Yang, et al., Adv. Mater. Interfaces (2019) 1901758.
[5] G. Zhou, B. Yao, Z. Xie, et al., Angew. Chem. Int. Ed. 46 (2007) 1149–1151.
[6] J. Ding, B. Wang, Z. Yue, et al., Angew. Chem. Int. Ed. 48 (2009) 6664–6666.
[7] D. Xia, B. Wang, B. Chen, et al., Angew. Chem. Int. Ed. 53 (2014) 1048–1052.
[8] C. Fan, C. Duan, H. Xu, et al., Chem. Mater. 27 (2015) 5131–5140.
[9] L. Zhao, S. Wang, S. Shao, et al., J. Mater. Chem. C 3 (2015) 8895–8903.
[10] F. Liu, H. Liu, P. Lu, et al., Nano Energy 68 (2020) 104325.
[11] C. Hippola, D. Danilovic, J. Shinar, Adv. Opt. Mater. 8 (2020) 0191282.
[12] M. Romain, D. Tondelier, B. Geffroy, et al., Chem. Eur. J. 21 (2015) 9426–9439.
[13] L. Sicard, C. Quinton, J.D. Peltier, et al., Chem. Eur. J. 23 (2017) 7719–7727.
[14] L. Sicard, C. Quinton, F. Lucas, et al., J. Phys. Chem. C 123 (2019) 19094–19104.
[15] J. Oniki, T. Moriuchi, T. Amaya, et al., J. Am. Chem. Soc. 141 (2019) 18238–18245.
[16] Y.H. Kim, D.C. Shin, S.K. Kwon, et al., Adv. Mater. 13 (2001) 1690–1693.
[17] J. Luo, Y. Zhou, J. Pei, et al., J. Am. Chem. Soc. 129 (2007) 11314–11315.
[18] Y.I. Park, J.H. Son, J.W. Park, et al., Chem. Commun. 18 (2008) 2143–2145.
[19] C. Poriel, L. Sicard, J. Rault-Berthelot, Chem. Commun. 55 (2019) 14238–14254.
[20] Z. Jiang, C. Yang, Y. Liu, et al., Adv. Funct. Mater. 19 (2010) 3987–3995.
[21] C. Poriel, J. Rault-Berthelot, Acc. Chem. Res. 51 (2018) 1818–1830.
[22] Y. Li, Z. Wang, X. Li, et al., Chem. Mater. 27 (2015) 1100–1109.
[23] M. Romain, D. Tondelier, B. Geffroy, et al., Chem. Commun. 51 (2015) 1313–1315.
[24] D. Xia, X. Guo, K. Müllen, et al., J. Mater. Chem. A 3 (2015) 11086–11092.
[25] M. Romain, S. Thiery, C. Poriel, et al., Angew. Chem. Int. Ed. 54 (2015) 1176–1180.